Characterising Viral Vectors for Gene Therapy Delivery Using Mass Spectrometry on Different Levels

Josh Smith[1], Corentin Beaumal[1], Silvia Millán-Martín[1], Sara Carillo[1], Aaron Richardson[1], Colin Clarke[1,2] & Jonathan Bones[1,2]

[1]NIBRT, Foster Avenue, Mount Merrion, Blackrock, Co. Dublin, A94 X099, Ireland.
[2]School of Chemical and Bioprocess Engineering, University College Dublin, Belfield, Dublin 4, D04 V1W8, Ireland.

nibrt

Capsid Fill State Assessment Using Native MS

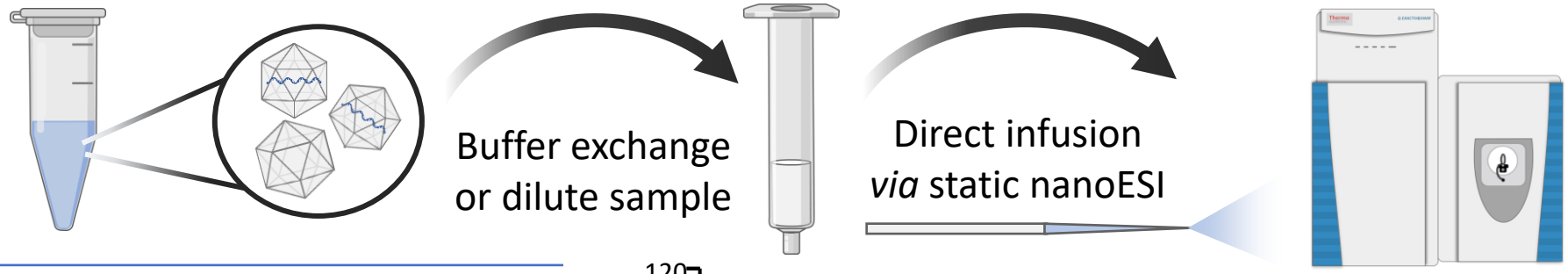

Thermo Q Exactive UHMR	Setting
Resolution	25,000 at m/z 200
Microscans	10
AGC Target	1e06
Max. IT	200 ms
In-source trapping	-100 V
Source DC offset	-50 V
Extended trapping	150 V
Trapping gas	SF_6 at 4e-10 mbar
Acquisition	5 mins with transient averaging enabled

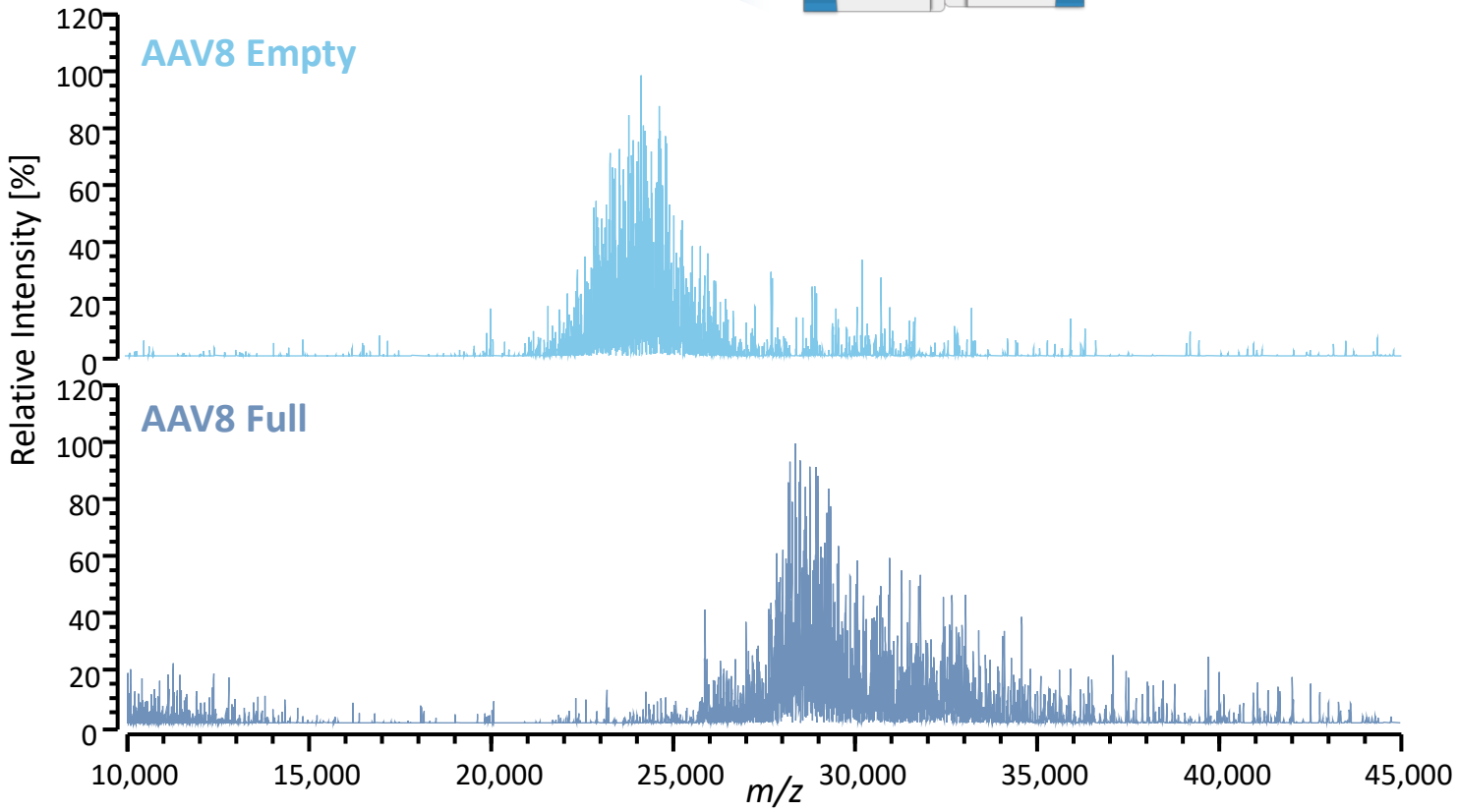

Coupling with Anion Exchange Chromatography

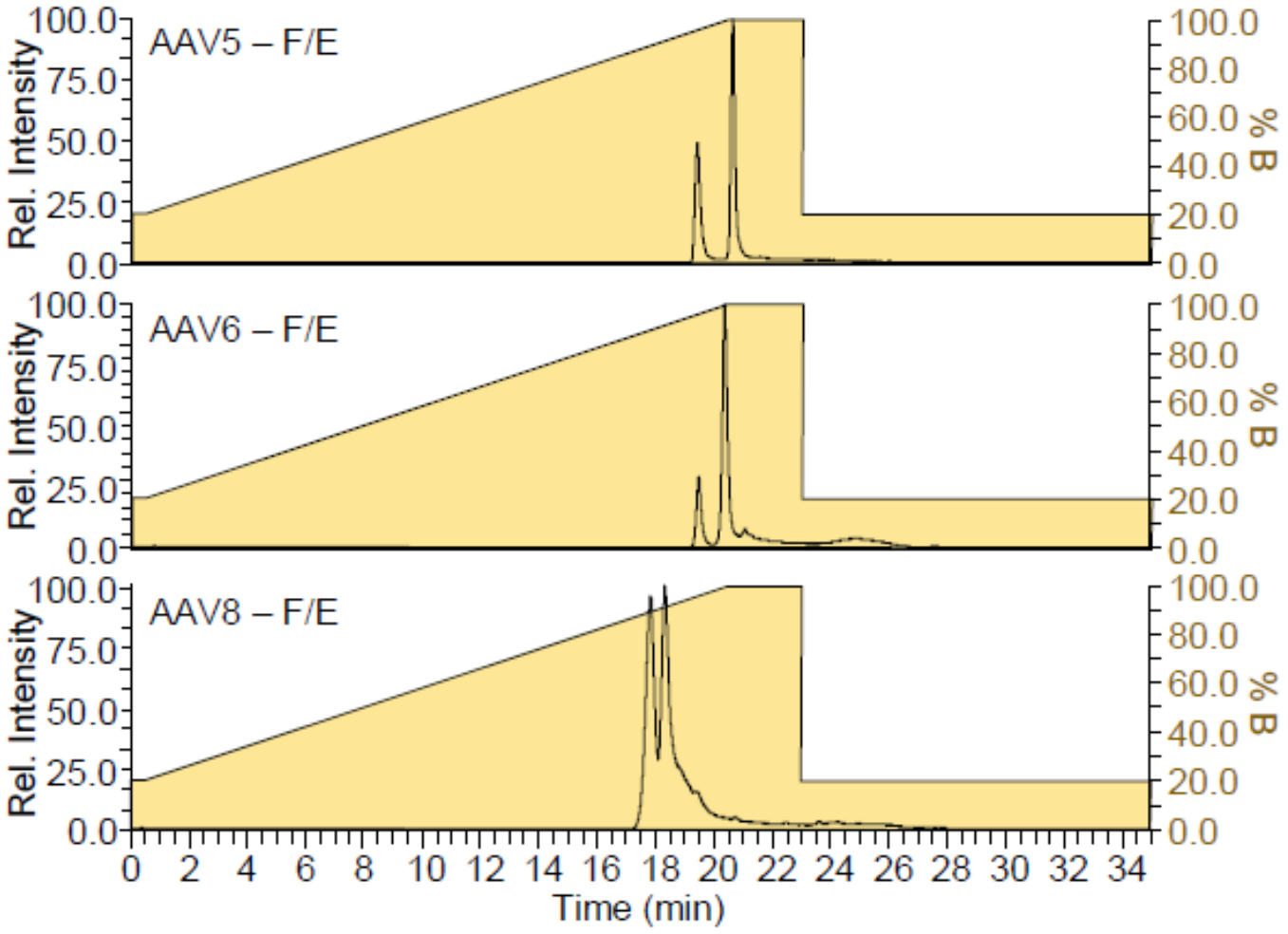

- pH gradient anion exchange separation of full and empty capsids using Thermo Scientific ProPac 3R AEX column.
- Gradient specifically designed to be generic for different serotypes and mass spectrometry compatible.
- pH gradients enable focusing effect, elution occurs when gradient pH = analyte pI, results in sharp chromatographic peaks.

Determination of Capsid Fill State Elution Order

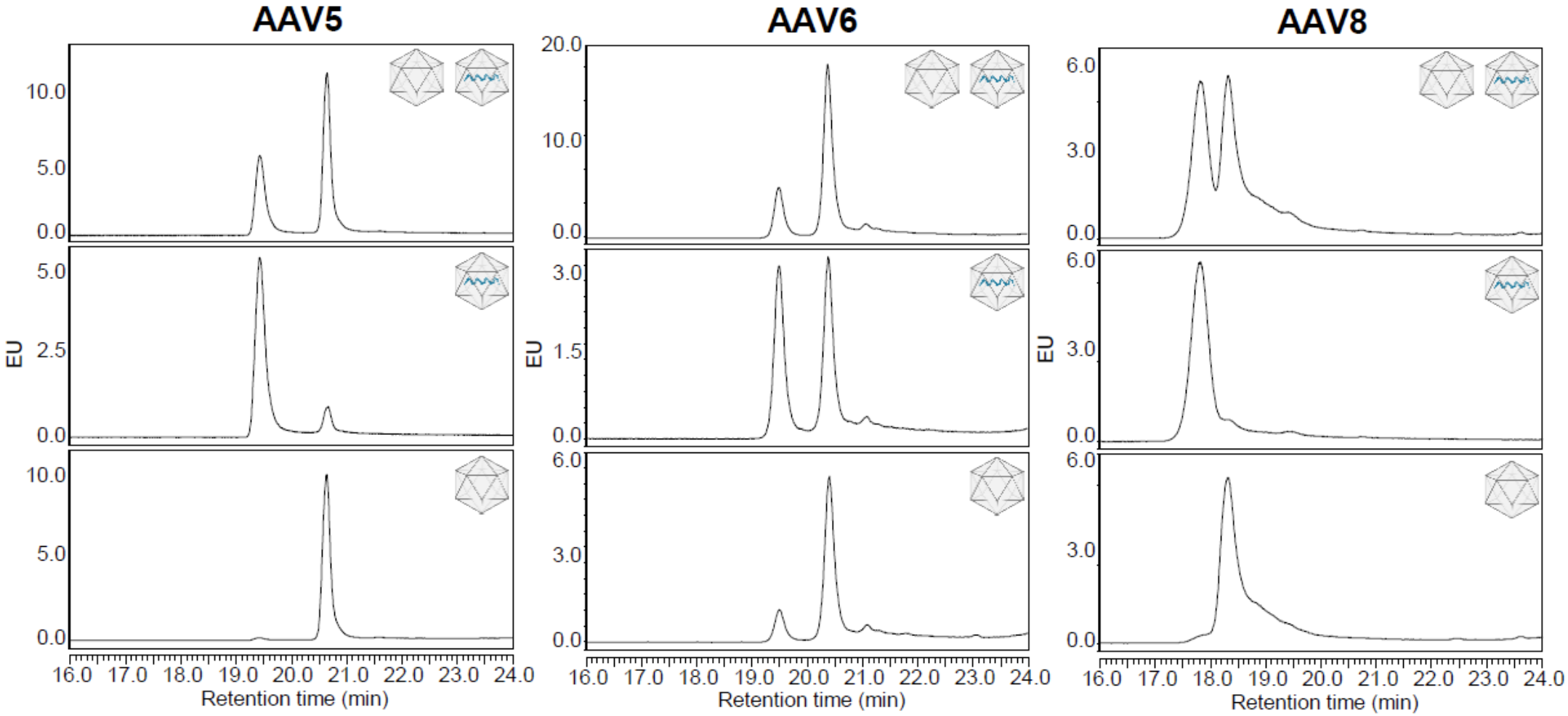

Coupling pH Gradient AEX with Native MS Detection

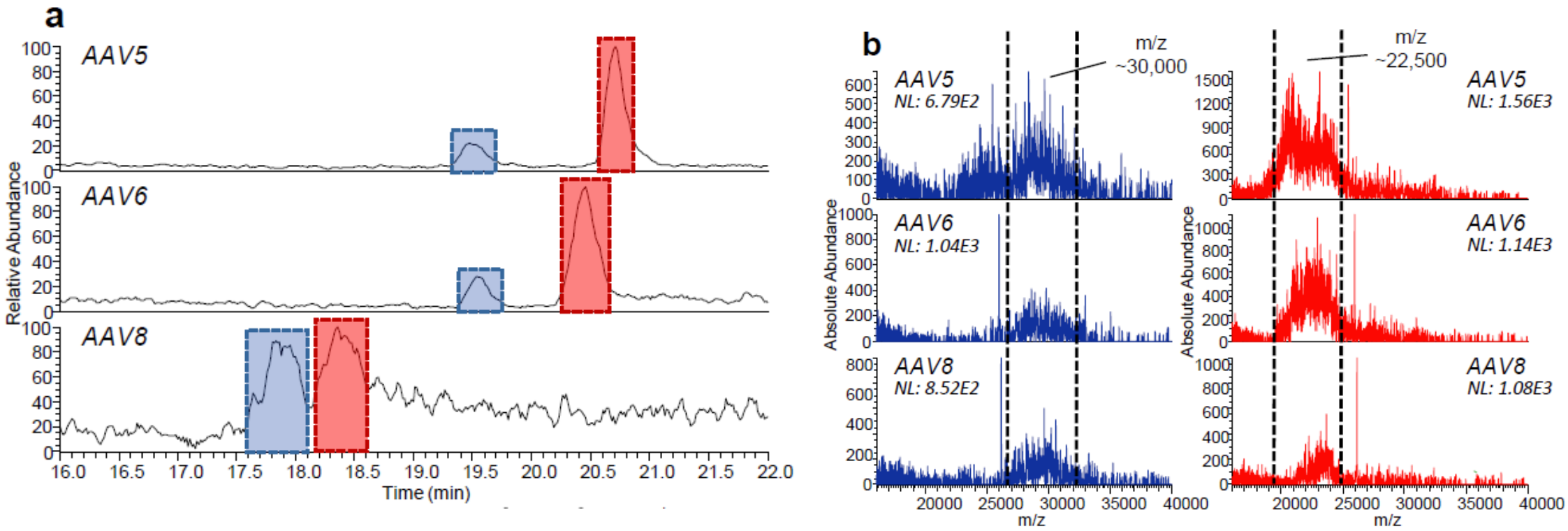

- pH gradient anion exchanged coupled directly to Thermo Scientific Q Exactive UHMR mass spectrometer for confirmation of capsid fill state species identification based on m/z.
- Assuming similar charge, earlier eluting peak contains heavier species explained by the presence of cargo DNA, additional mass of ~0.8 MDa corresponding to CMV-GFP.

Coupling pH Gradient AEX with Charge Detection MS

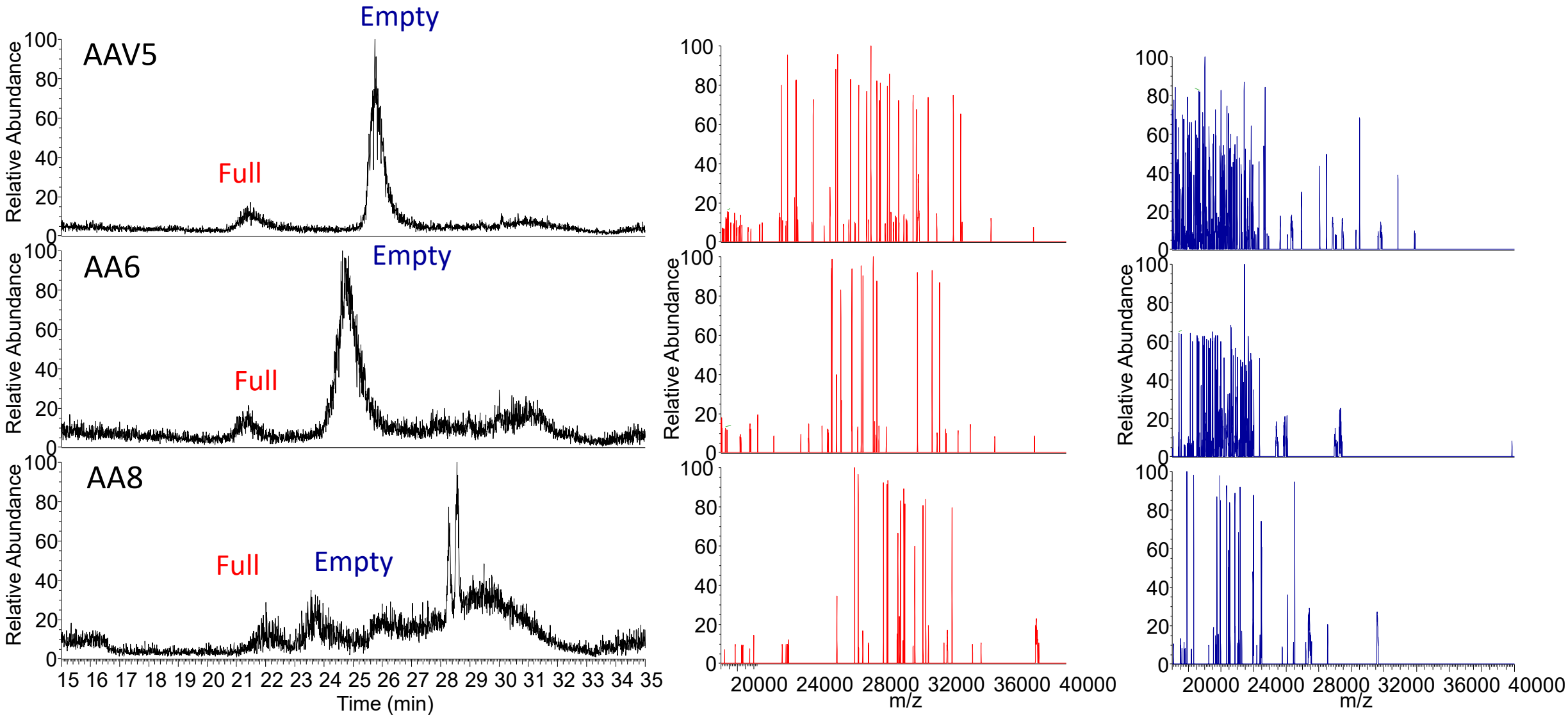

Viral Protein Separation using LC-MS

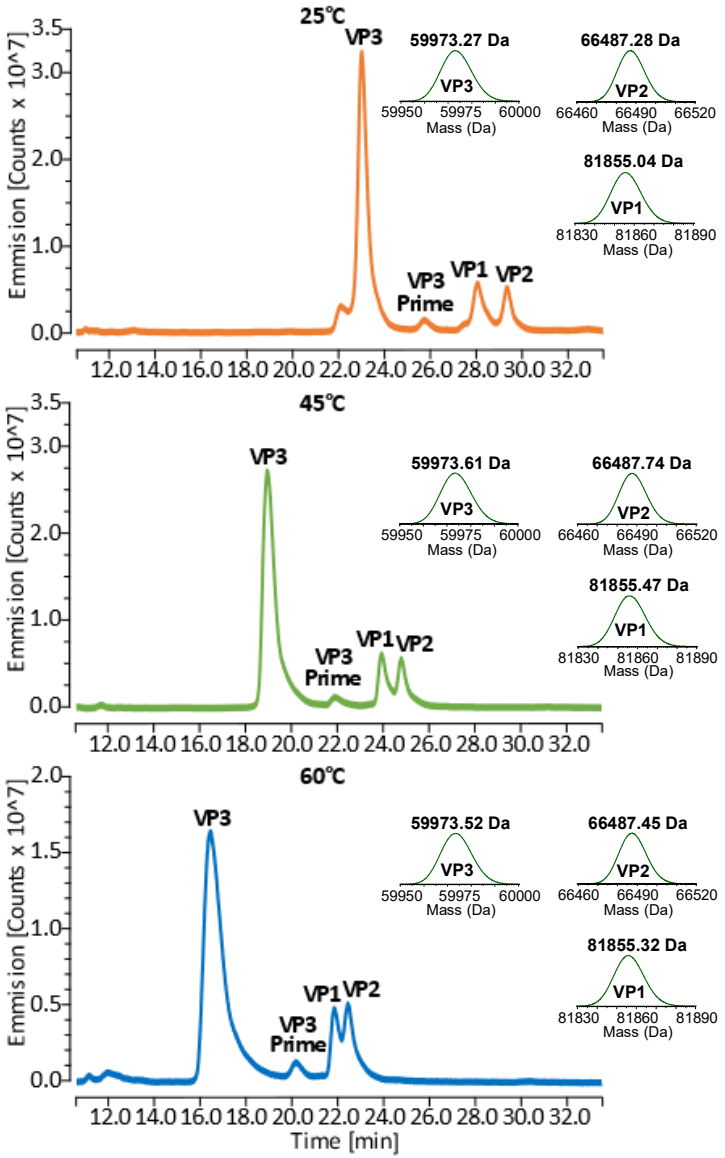

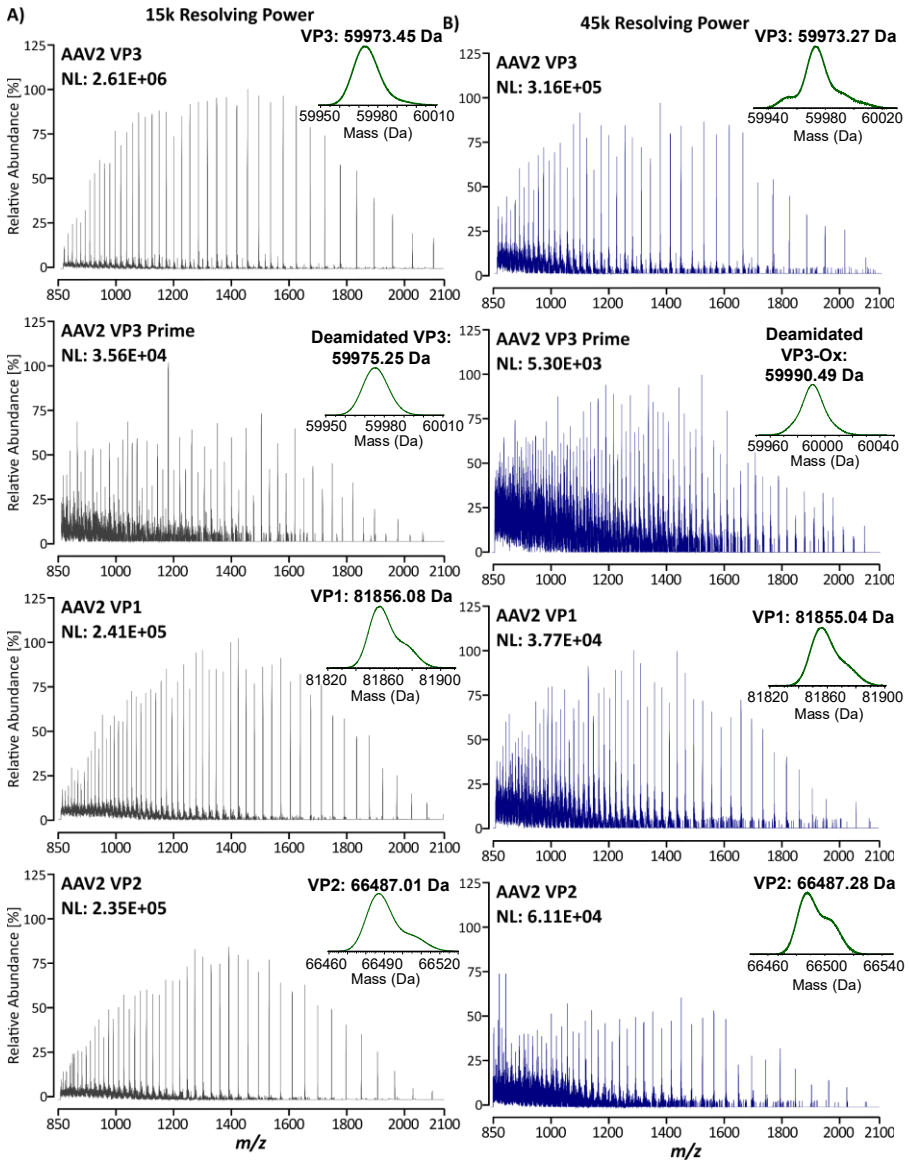

- VP separation using hydrophilic interaction LC using an acetonitrile water gradient containing difluoro acetic acid as a mobile phase modifier.
- Fluorescence and MS detection using Thermo Scientific Orbitrap Exploris 240 MS with Biopharma Option.

Method Translation into Rapid Identity Test

Component Identification

BioPharma Finder Software 4.1

Processing Method and Component List Importation from BPF

Intact Protein Deconvolution

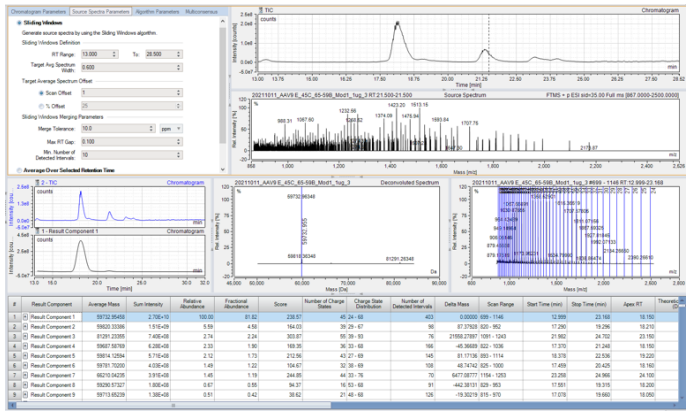

Serotype Profiling

Data Processing Parameter Optimization (Sf9 Derived AAVs)

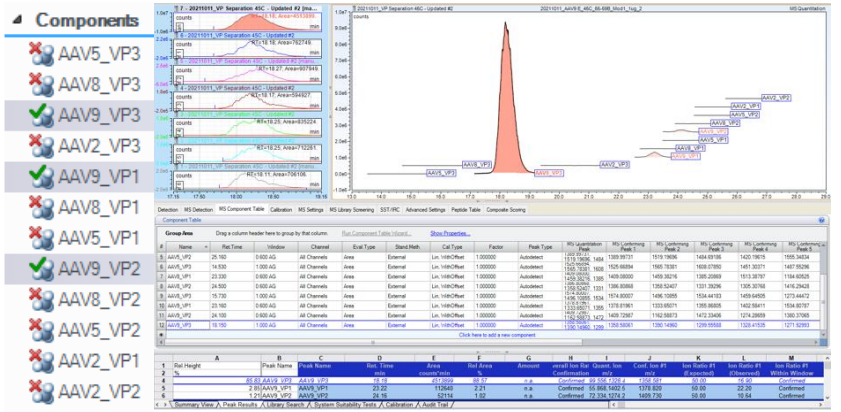

Report Generation

Specific Serotype PTM Monitoring

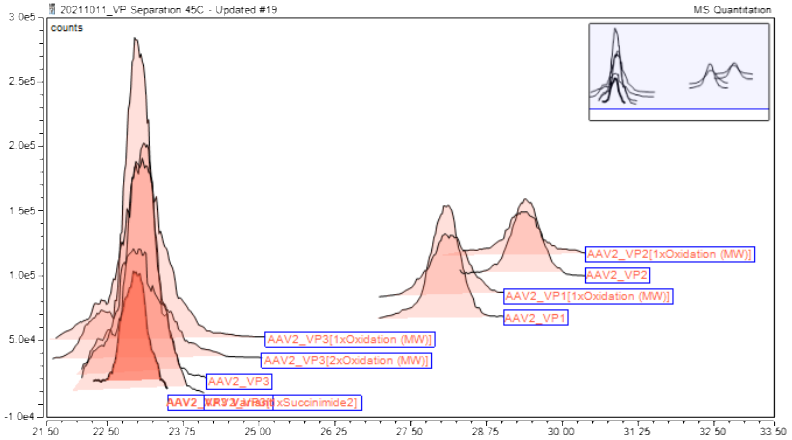

Method Validation (HEK Derived AAV)

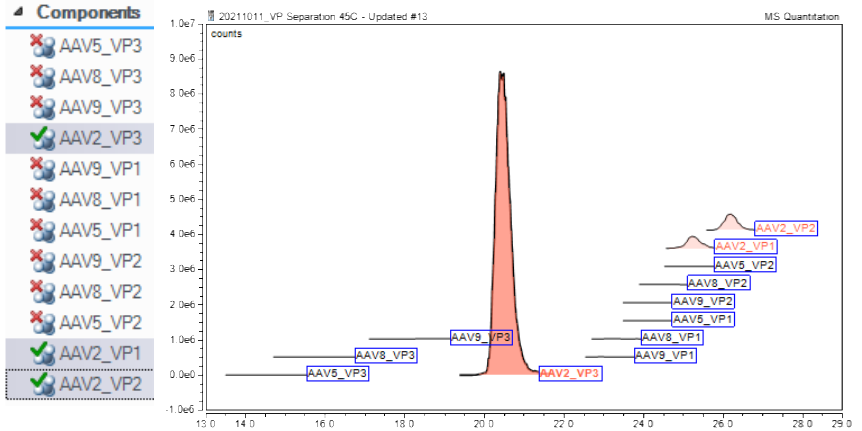

Viral Protein Separation using MCE-MS

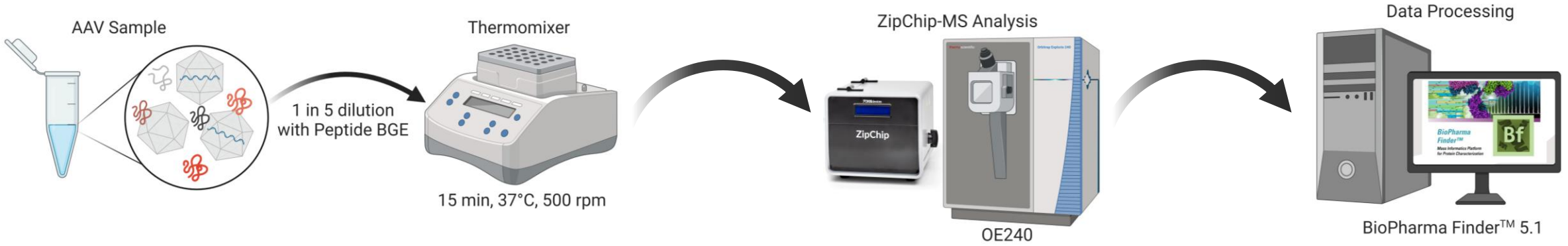

Empty vs. Full Profiles

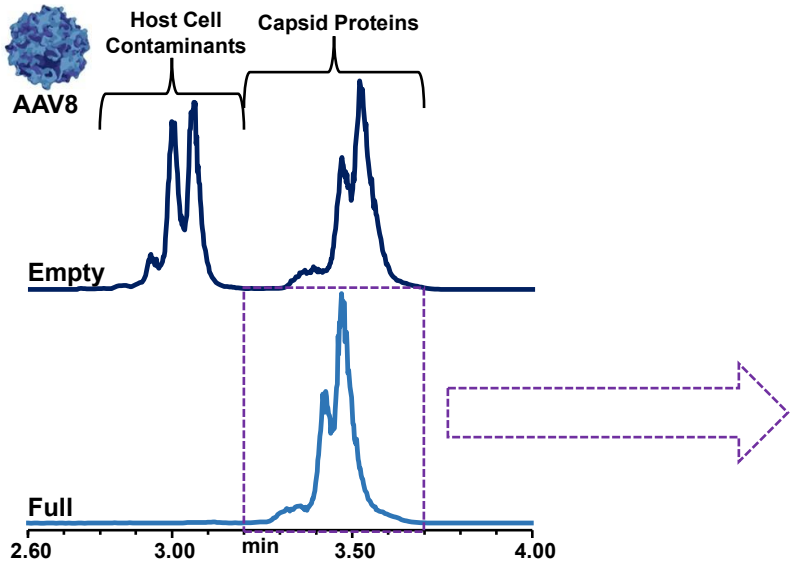

VP Proteoform Characterization

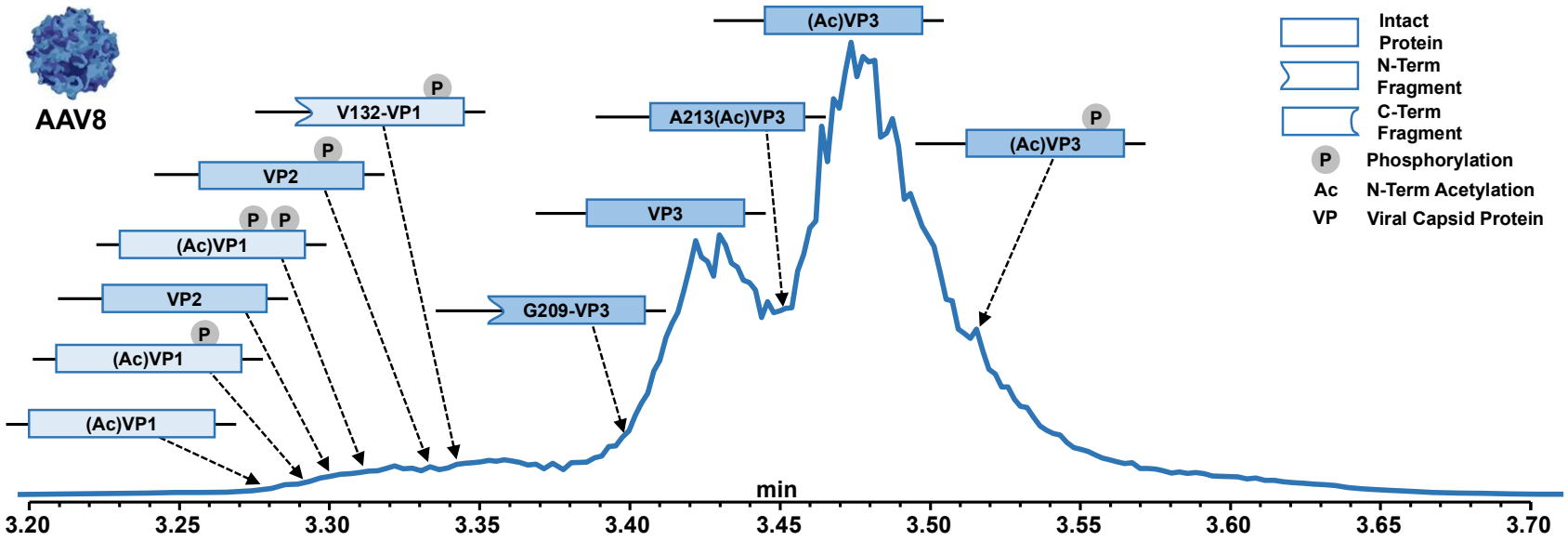

Broad Applicability of ZipChip Platform

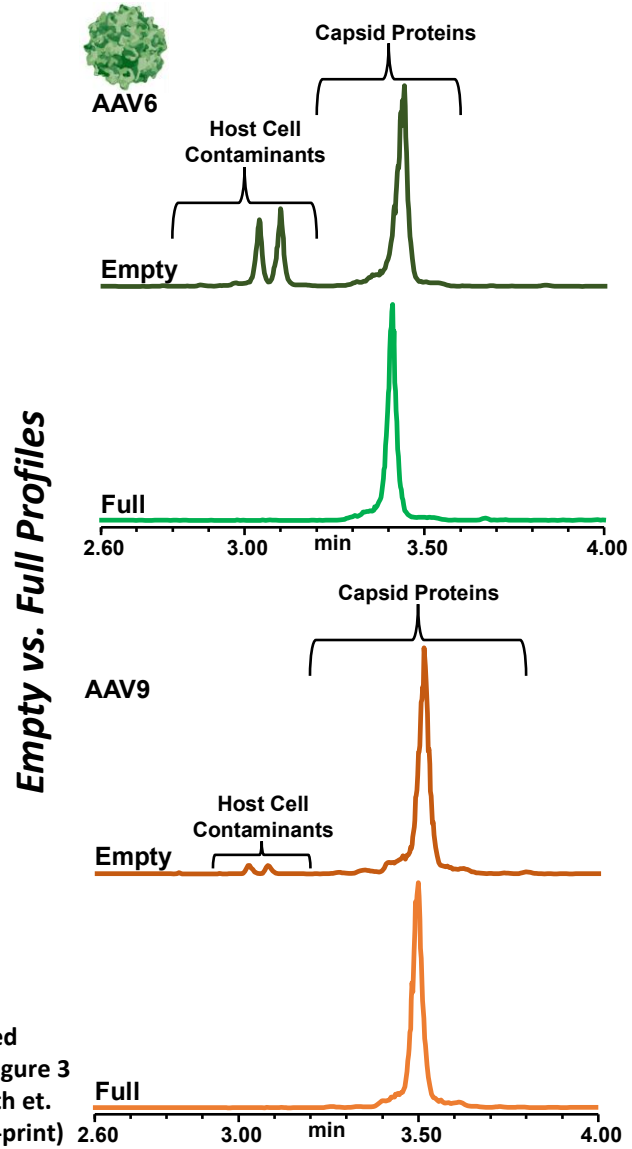

Adapted from Figure 3 of Smith et. al (Pre-print)

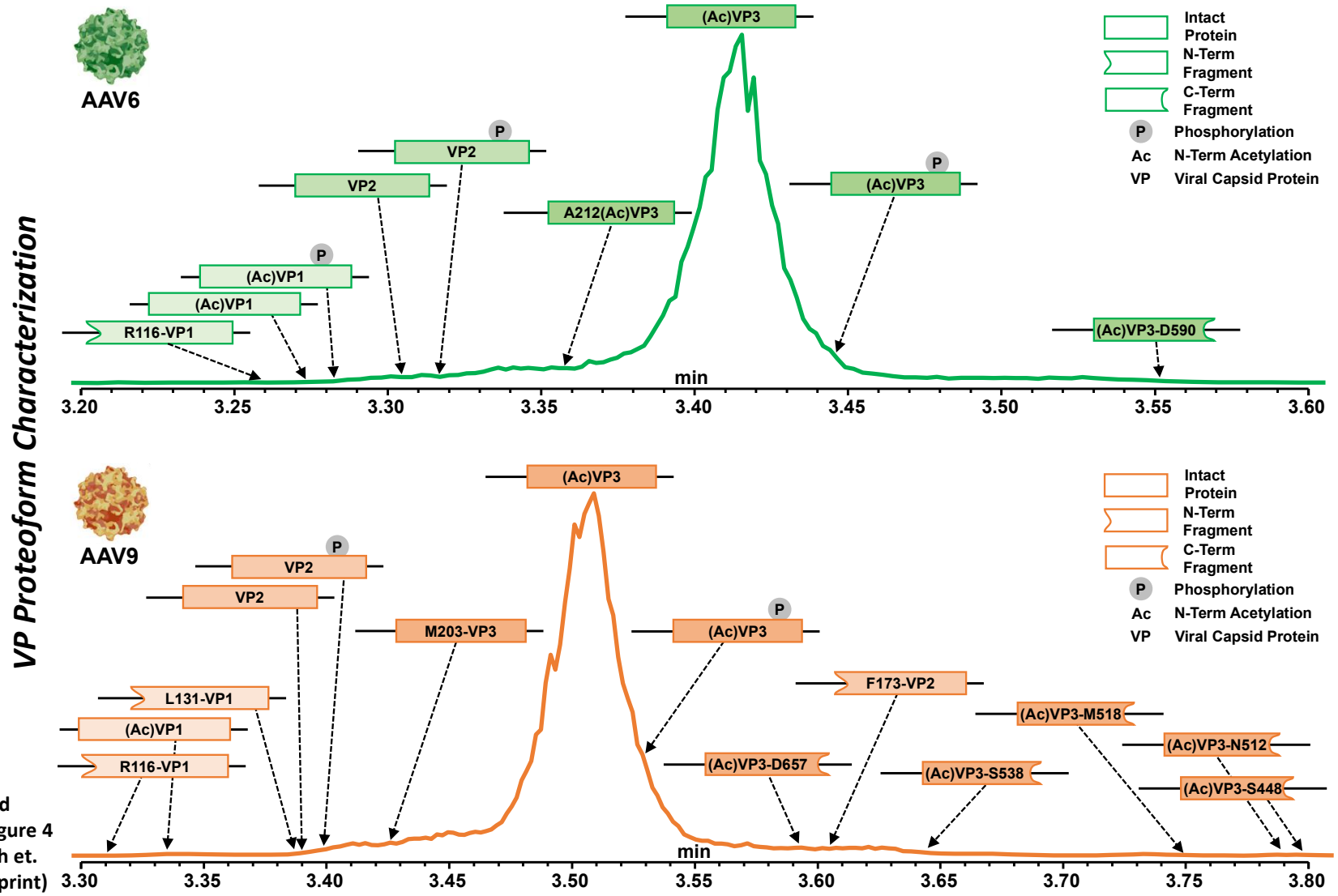

Adapted from Figure 4 of Smith et. al (Pre-print)

Detected VP Proteoforms and Fragments

Start of AAV Sequence

Expected VPs

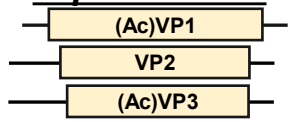

VP3 Variant

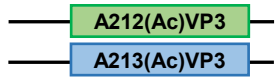

N-Term Fragments

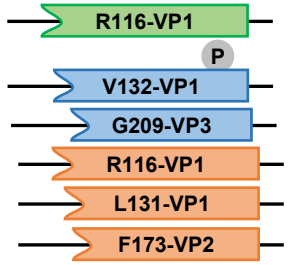

VPs with additional PTMs

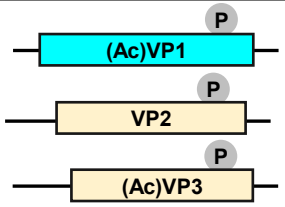

C-Term Fragments

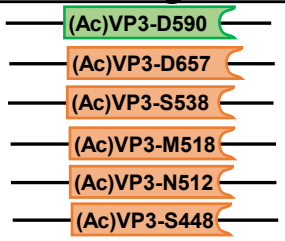

Unexpected VPs

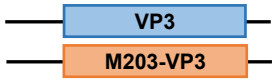

Potential Causes of Fragments

- Baculoviral cathepsin
- Immune response
- Acidic conditions

VP3 Variant Generation

Serotypes	N-terminal region 203	211	DP sequence 590 591	DG sequence 626 627	DP sequence 656 657
AAV1	... M A S G G G A P M A ...		T D P A ...	T D G H ...	A N P P ...
AAV2	... M A T G S G A P M A ...		R Q A A ...	T D G H ...	A N P S ...
AAV3	... M A S G G G A P M A ...		T A P T ...	T D G H ...	A N P P ...
AAV6	... M A S G G G A P M A ...		T D P A ...	T D G H ...	A N P P ...
AAV8	... M A A G G G A P M A ...		T A P Q ...	T D G N ...	A D P P ...
AAV10	... M A A G G G A P M A ...		T G P I ...	T D G N ...	A D P P ...
AAVrh10	... M A A G G G A P M A ...		A A P I ...	T D G N ...	A D P P ...
AAV4	... M R A A A G G A A V ...		N L P T ...	T D G H ...	A N P A ...
AAV11	... M R A A P G G N A V ...		T A P I ...	A D G H ...	A N P A ...
AAV12	... M R A A P G G N A V ...		T A P H ...	T D G H ...	A N P N ...
AAV5	... M S A G G G G P L G ...		T A P A ...	T G A H ...	G N I - ...
AAV9	... M A S G G G A P V A ...		A Q A Q ...	T D G N ...	A D P P ...
AAV7	... V A A G G G A P M A ...		T A A Q ...	T D G N ...	A N P P ...

Adapted from Figure 5a of *Oyama et al. (2021)*
https://www.liebertpub.com/doi/10.1089/hum.2021.009

"Leaky" Codon Scanning

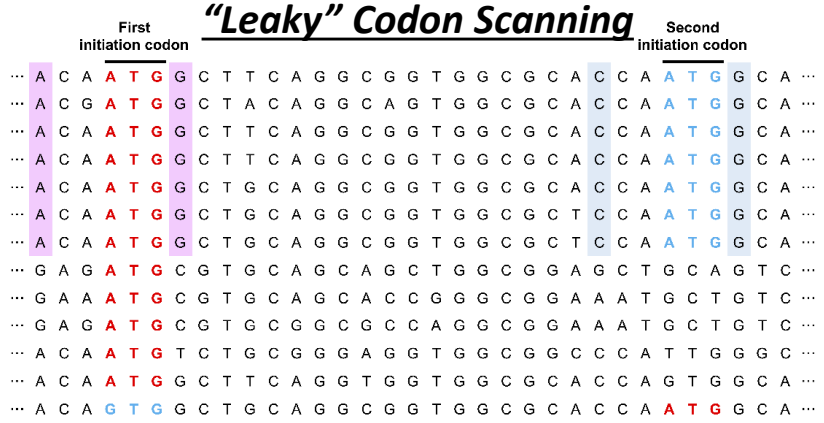

Adapted from Figure S4a of *Oyama et al. (2021)*
https://www.liebertpub.com/doi/10.1089/hum.2021.009

Key

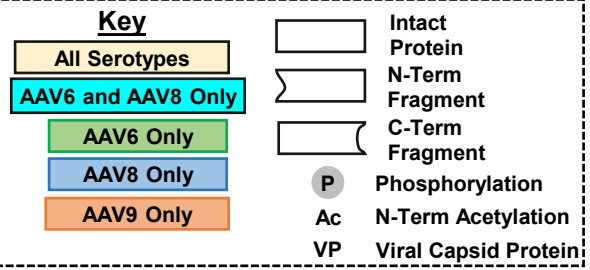

RP LC-MS/MS for Detection of Deamidation Events

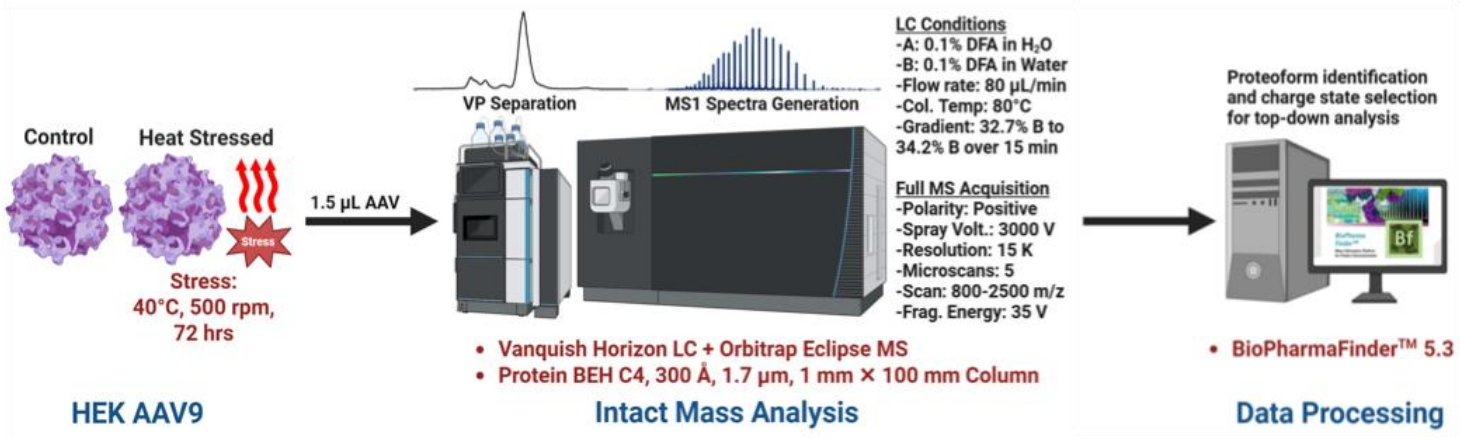

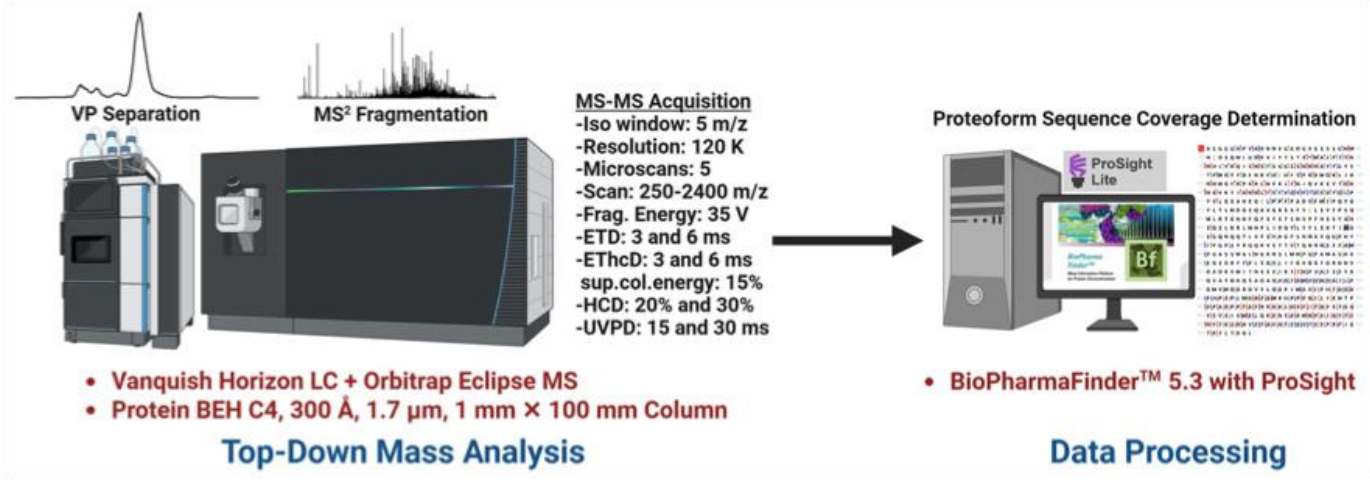

While the HILIC separation of VP's works well, for modifications such as deamidation events, HILIC does not have the necessary selectivity. Reversed-phase separation on C4 enables efficient separation of deamidated forms of the viral proteins.

RP LC-MS/MS for Detection of Deamidation Events

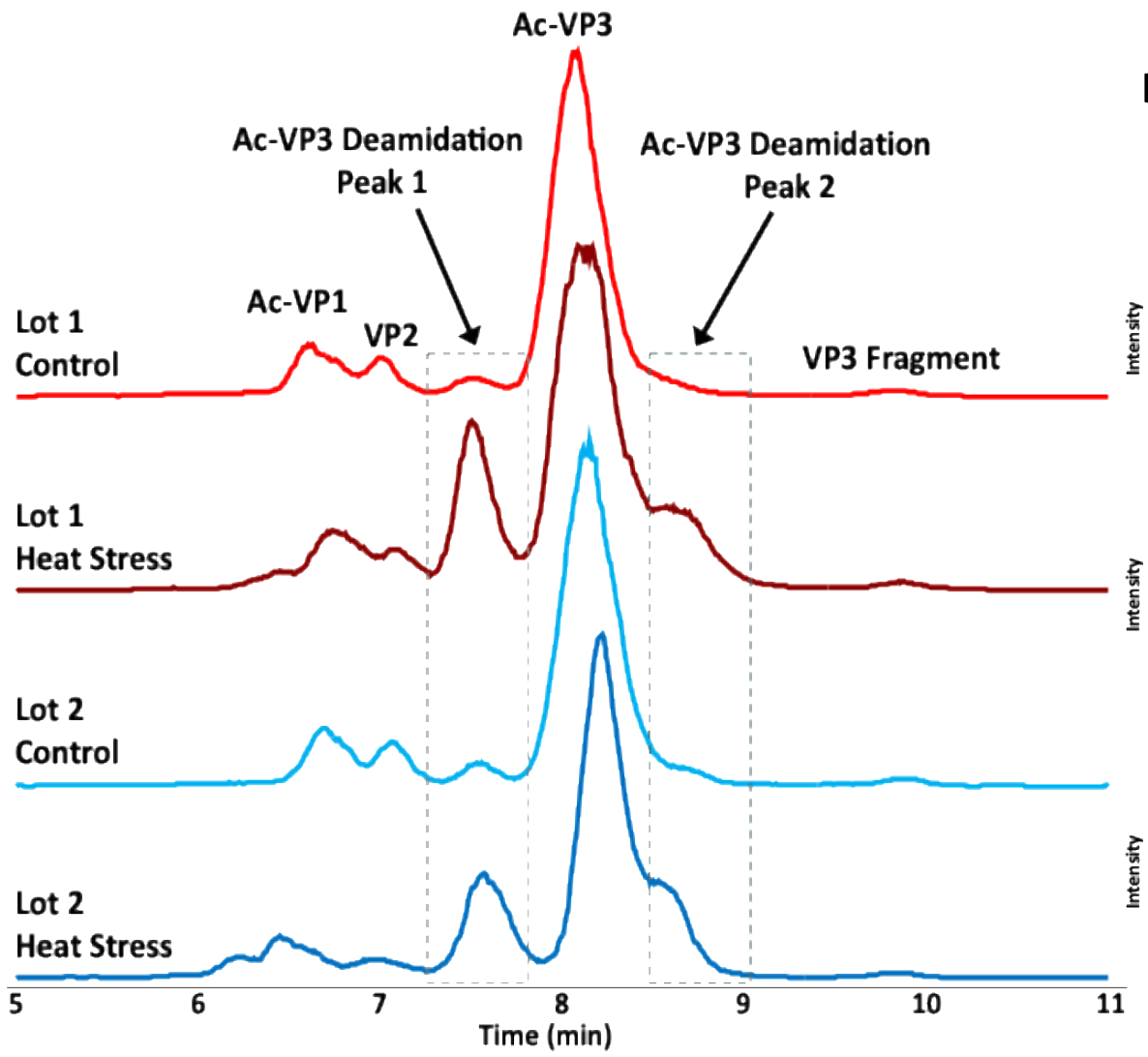

For deamidation events, HILIC does not have the necessary selectivity. C4 RP LC-MS enables efficient separation of deamidated forms of VPs.

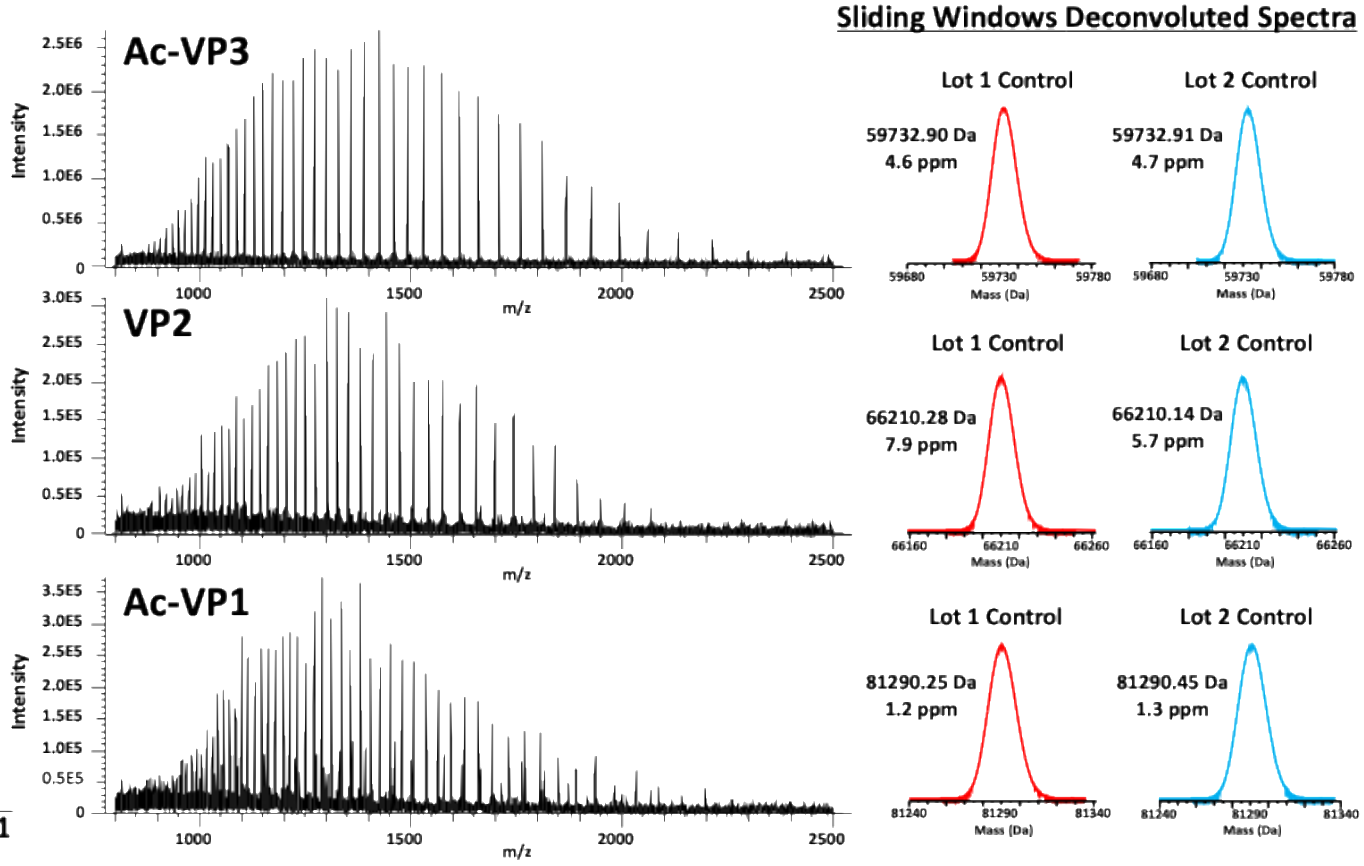

Top-Down LC-MS/MS Using Different Ion Activation

Selected Precursor Ions for MS/MS Fragmentation

	ETD & EThcD		HCD & UVPD	
Compound	m/z	z	m/z	z
VP1	1004.21	66	1084.86	75
VP2	1004.21	60	1068.91	62
VP3	996.54	51	1107.17	54

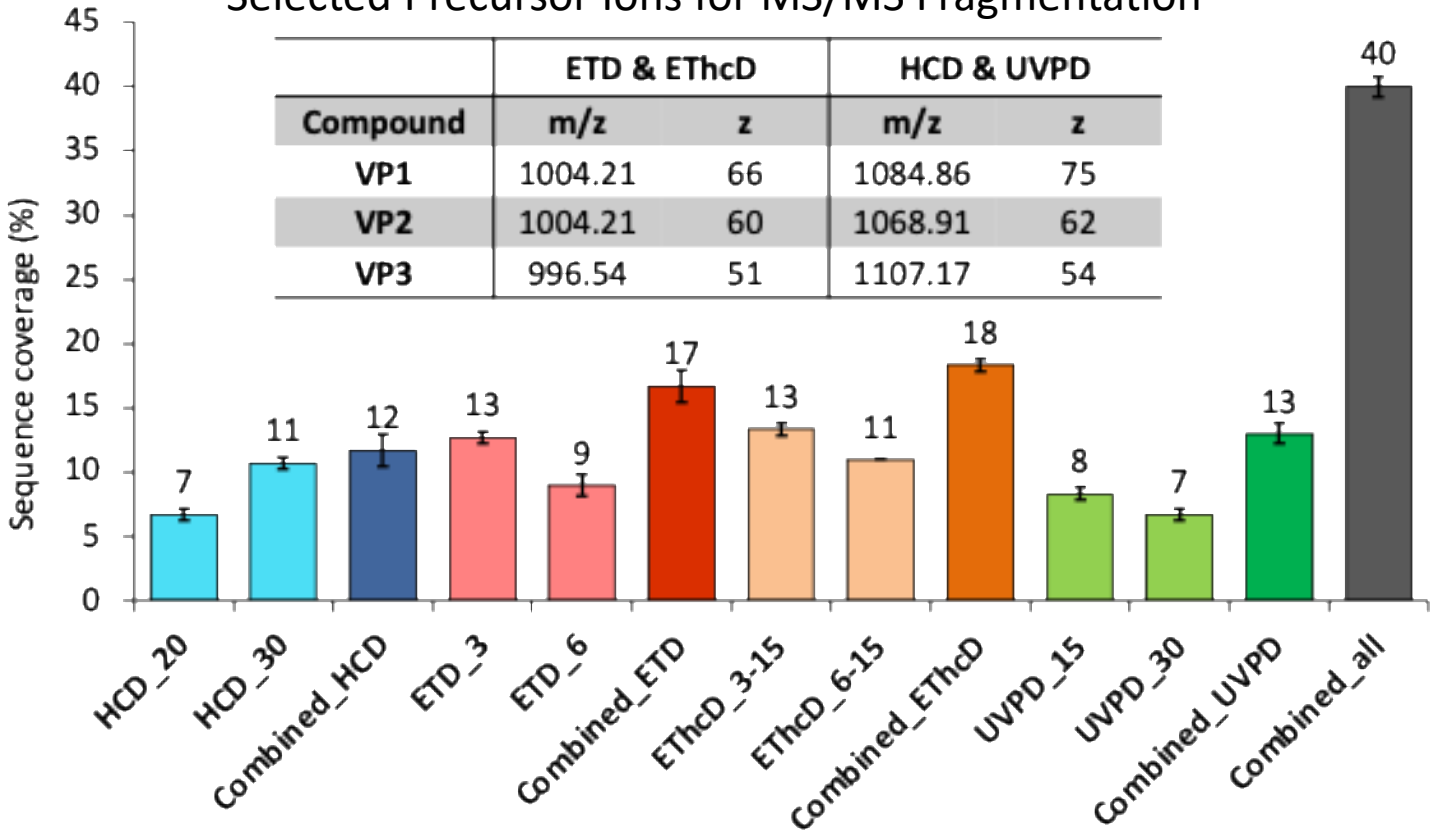

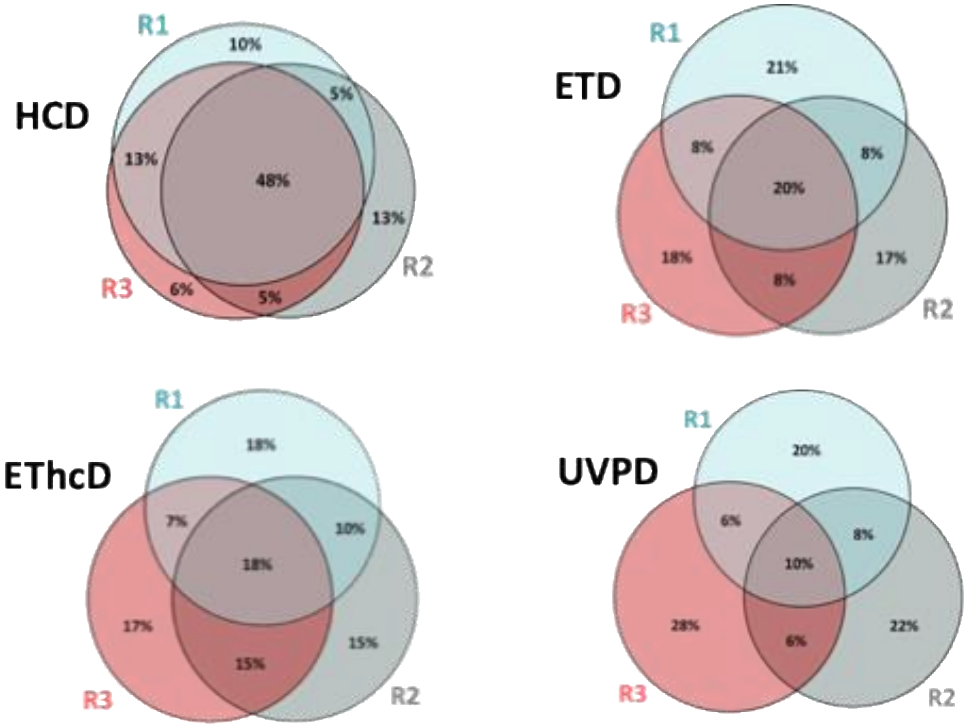

For deamidation events, HILIC does not have the necessary selectivity. C4 RP LC-MS enables efficient separation of deamidated forms of VPs.

Combined Top-Down MS/MS of VP3 on Orbitrap Eclipse

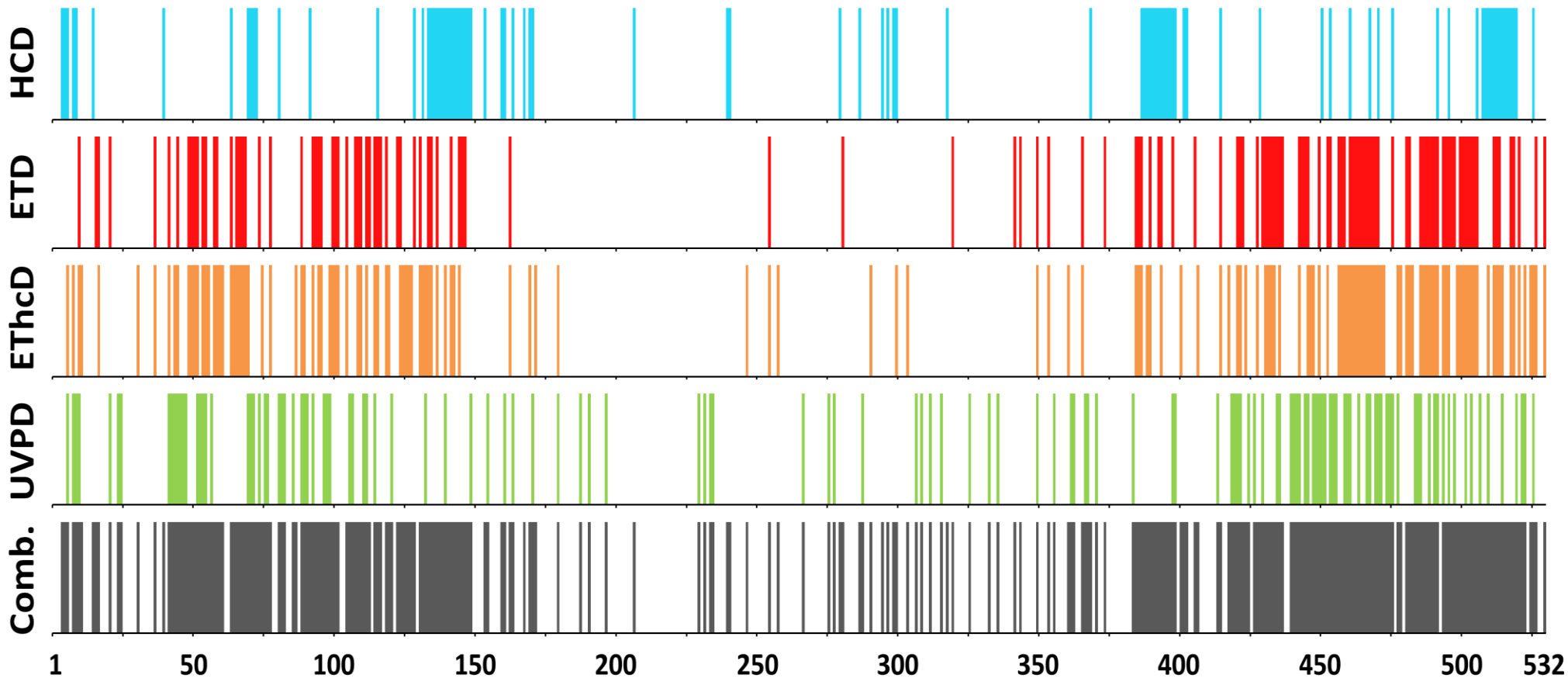

Bar code map depicting the fragmentation location in the amino acid sequence of the fragments detected in all fragmentation strategies using all replicates (n=12).

Top-down MS/MS Data Sequence Map of Deamidated VP3

Residue #	Peptides	Lot 1 Ctrl (%)	Lot 1 Heat Stress (%)	Lot 2 Ctrl (%)	Lot 2 Heat Stress (%)
N56+Deamidation (VP1 only)	YLGPGNGLDKGEPVNAADAAALEHDK (Y51-K76); YLGPGNGLDK (Y51-K60); YLGPGNGLDKGEPVNAADAAALEHDKAYDQQLK (Y51-K83)	14.28	**41.80**	15.87	**47.60**
N451+Deamidation (VP3:N249)	TINGSGQNQQTLK (T449-K461)	3.15	**33.34**	8.55	**39.97**

Peptide mapping identified N249 as a deamidation site.
Top-down MS/MS of the Ac-VP3-DP1 peak also enabled identification of the deamidated residue.
Overall performance of top-down LC-MS/MS is dependant on the abundance of the proteoform under study.

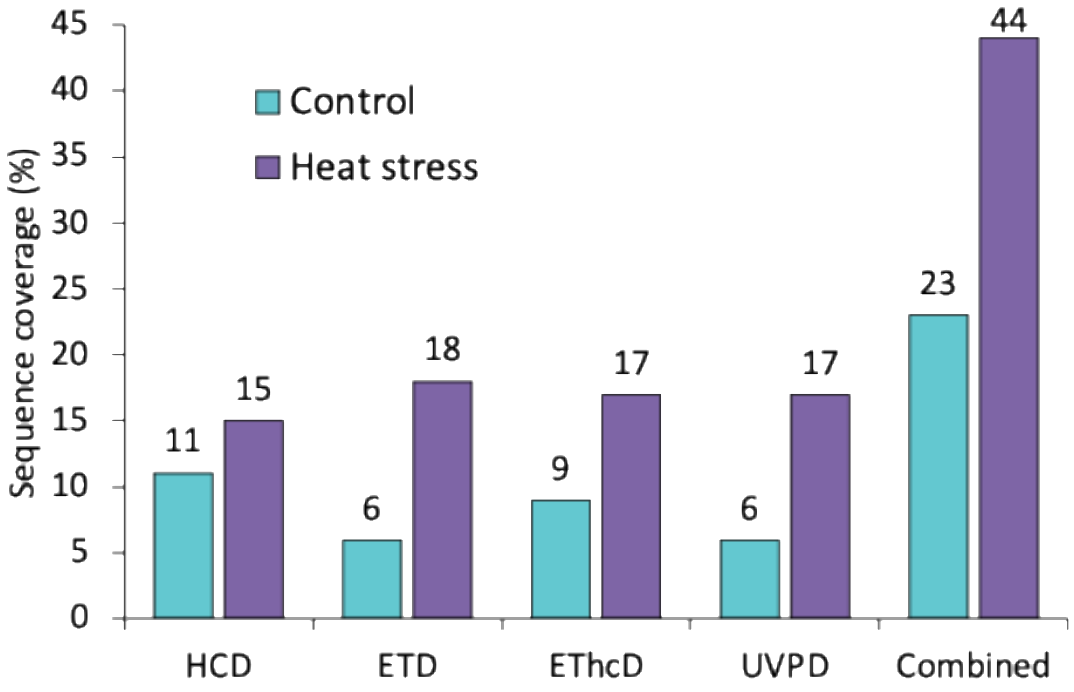

HCP Analysis Using Orbitrap Astral LC-MS

The Thermo Scientific™ Orbitrap™ Astral™ MS - Powered by the synergy of two synchronized HRAM analysers

ORBITRAP ANALYZER for high dynamic range HRAM MS and MS/MS	
HRAM Scan Rate	Up to 40 Hz
Intrascan dynamic range	>5000 with single microscan
Max Resolution	480,000 at *m/z* 200
Mass Accuracy	RMS <3 ppm
Max *m/z* range	Up to *m/z* 8000 with Biopharma Option

ASTRAL ANALYZER for fast and sensitive high dynamic range HRAM SIM and MS/MS	
Sensitivity	Single ion detection
HRAM Scan Rate	Up to 200 Hz
Intrascan dynamic range	>1000 with single microscan
Resolution	80,000 at *m/z* 524
Mass Accuracy	RMS <5 ppm

Sample Preparation Workflow

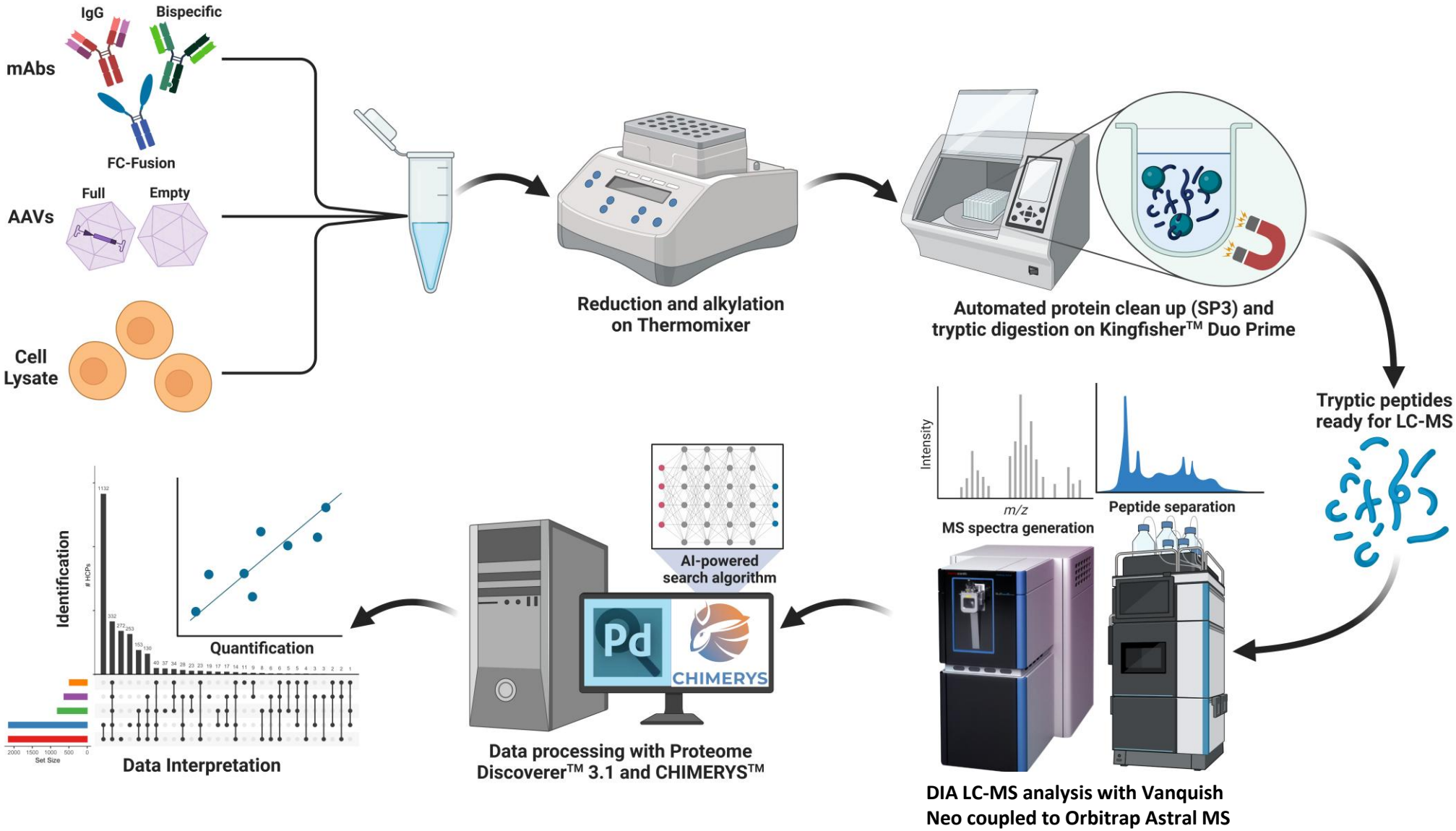

Tracking HCP Clearance using AAVX Affinity Chromatography

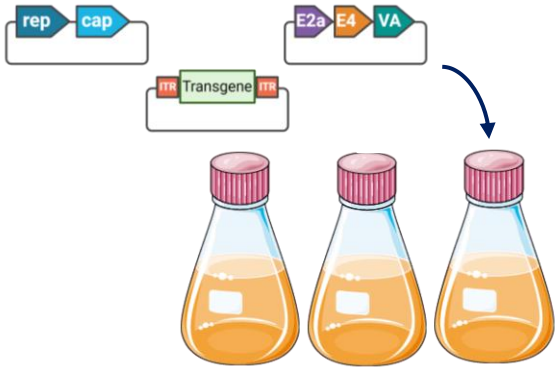

AAV produced in HEK cells using GIBCO AAV-MAX platform

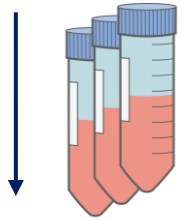

Conditioned media collected, sample retained, remainder purified using POROS CaptureSelect™ AAVX Affinity Resin pre-packed column

FPLC

Purified AAV buffer exchanged to PBS containing 0.01% Pluronic using centrifugal filters

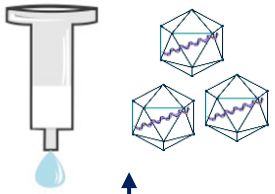

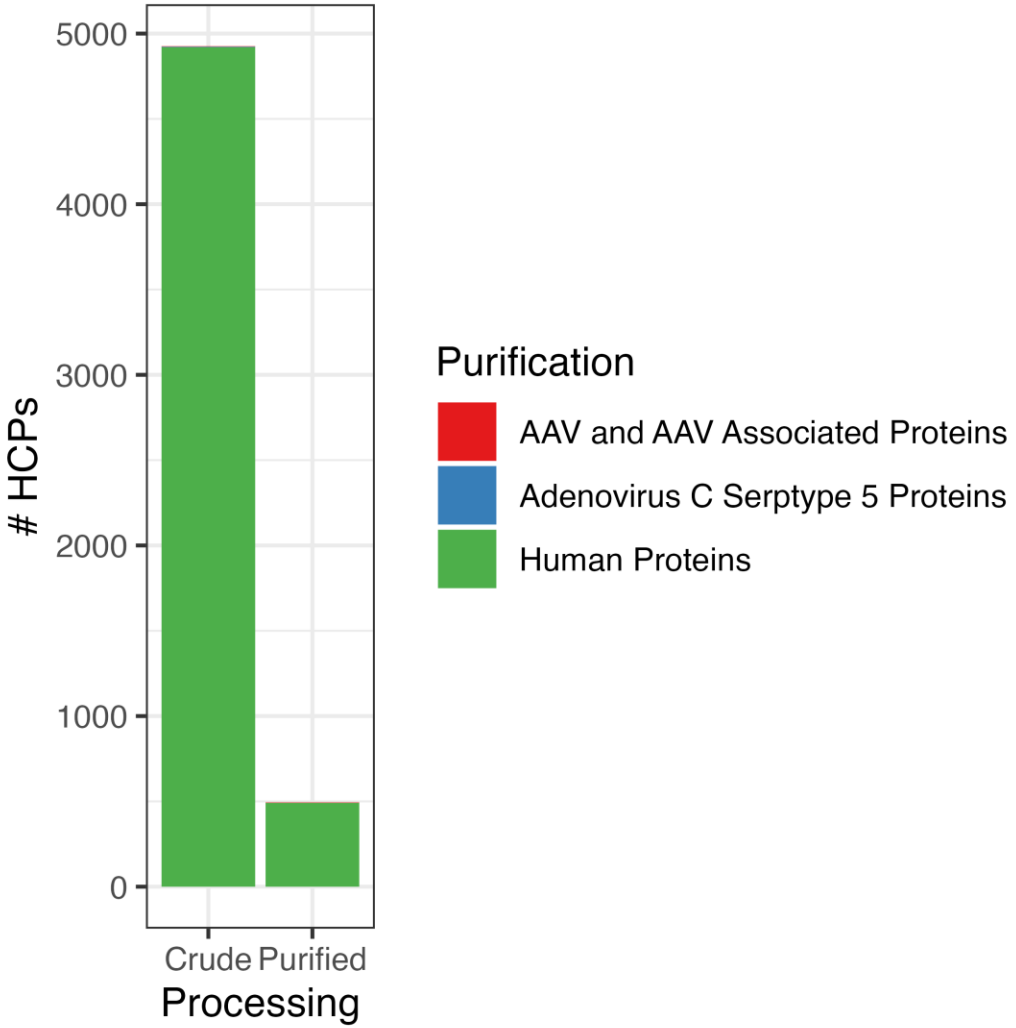

HCPs Associated with Purified CMV-GFP AAV8

- AAVX purification resulted in ~80% reduction in the levels of HCPs present in the process stream using a simple bind and elute method.
- For proteins associated with the retained viral capsids, GO terms relating to binding, in particular protein binding (92.7% of the total set) were enriched. 97.1% were mapped as being intracellular proteins.
- Standard physiochemical parameters were explored including molecular mass, pI, hydrophobicity *etc.* However, distributions were broad and as expected, no correlation existed.

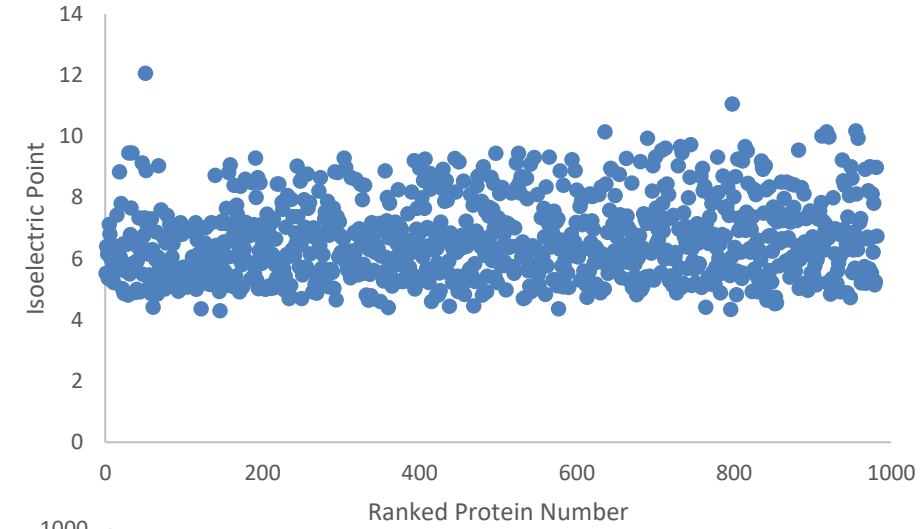

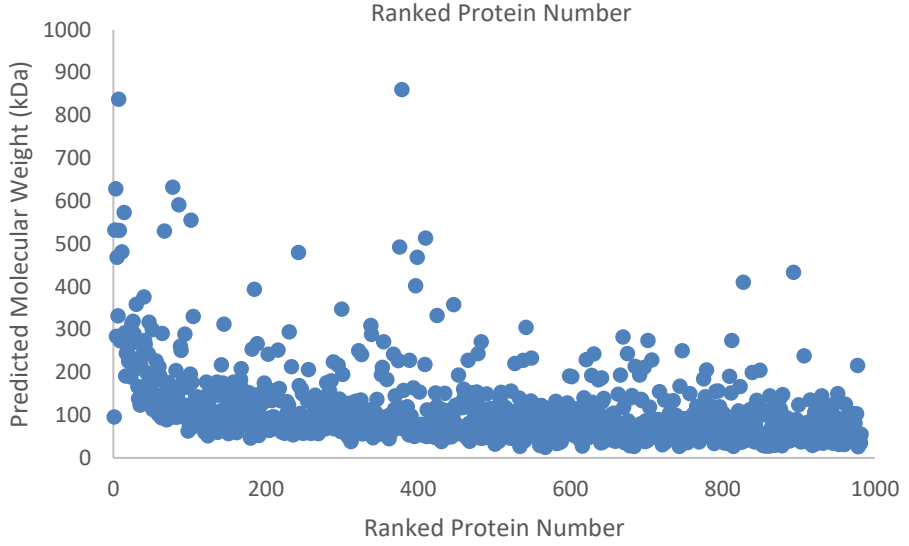

Exploring HCP Distribution Across Various AAV Serotypes

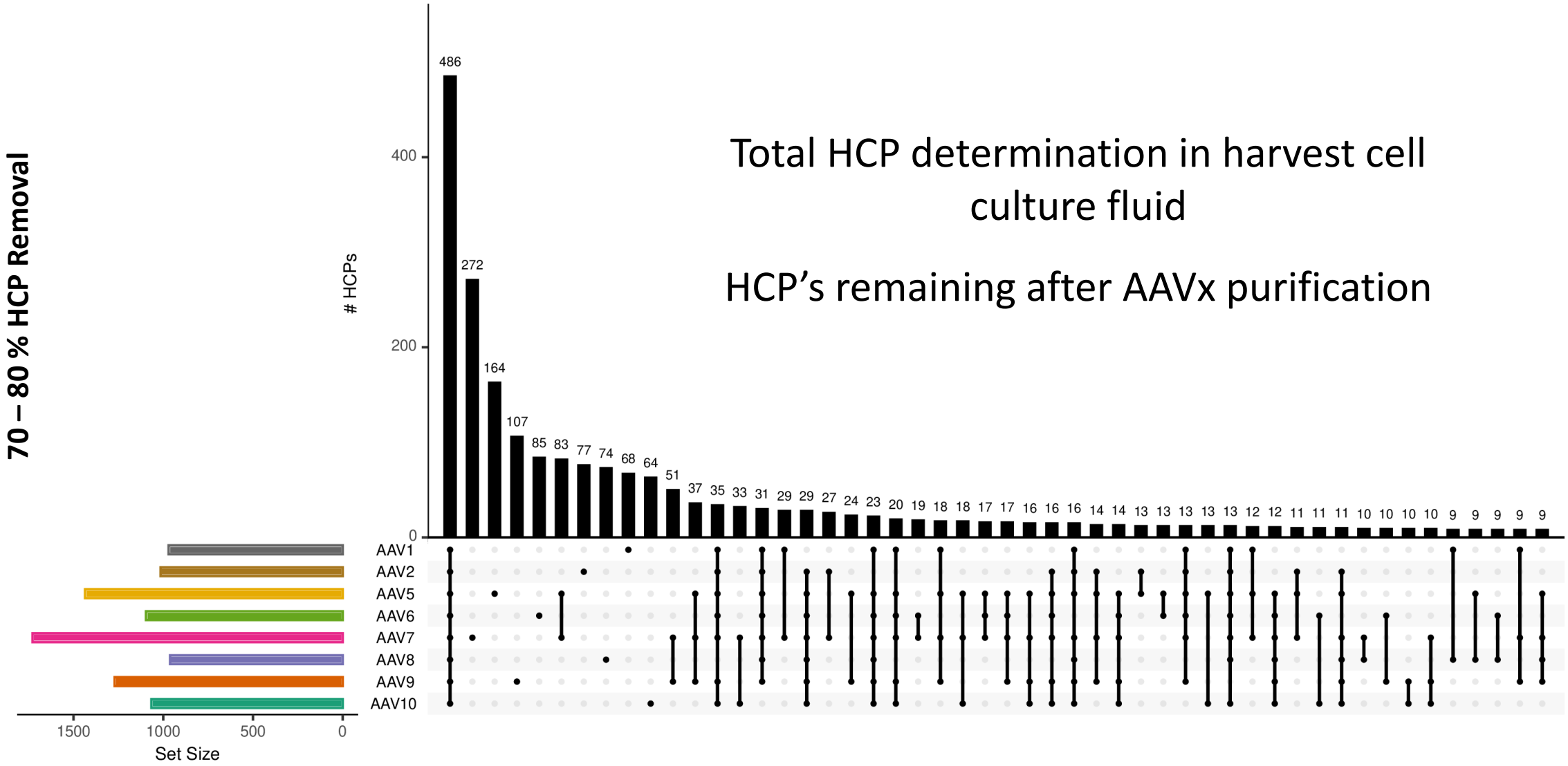

Total HCP determination in harvest cell culture fluid

HCP's remaining after AAVx purification

Monitoring Clearance Using Two-Step Downstream Processing

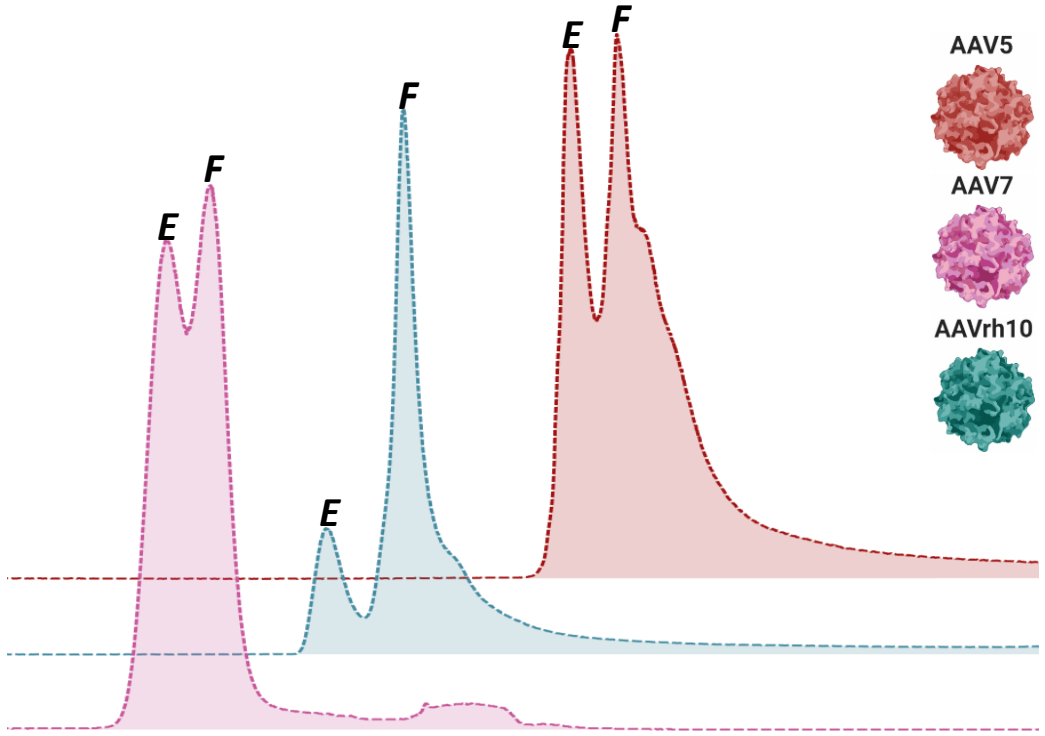

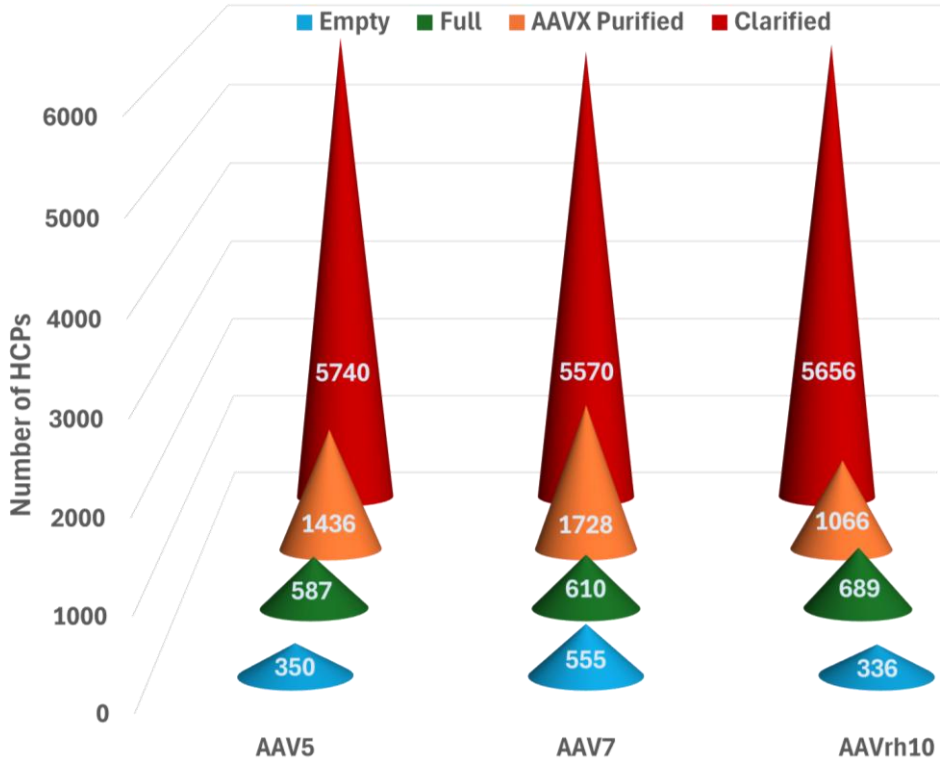

Post AAVX affinity purification, anion exchange separation of empty and full capsids were performed using Poros XQ. Fractions were collected and analysed by LC-MS on Orbitrap Astral to investigate clearance of the HCPs and distribution across the different capsid fill states.

Distribution of HCPs across Empty and Full Capsids

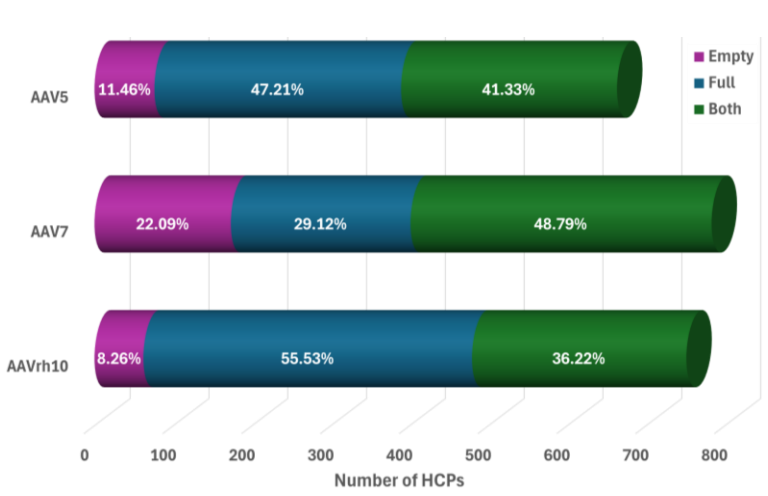

Potentially Harmful HCPs	Clarified			AAVX Purified			Empty			Full		
	AAV5	AAV7	AAVrh10	AAV5	AAV7	AAVrh10	AAV5	AAV7	AAVrh10	AAV5	AAV7	AAVrh10
Heat shock 70 kDa protein 1B	9345.64	9533.52	8595.08	23.49	38.43	15.14	4.68	3.21	2.69	3.34	1.78	2.61
Heat shock protein HSP 90-alpha	2457.25	2392.91	1184.63	7.12	7.92	0.60	0.14	0.25	0.14	0.18	0.54	0.27
Heat shock protein HSP 90-beta	1016.23	1018.65	2064.89	2.81	5.20	2.78	0.19	0.18	0.49	0.17	0.25	0.65
Heat shock cognate 71 kDa protein	736.99	705.87	629.43	3.90	2.07	0.82	0.44	0.36	0.44	0.67	0.36	0.51
60 kDa heat shock protein, mitochondrial	561.73	519.28	544.00	0.66	1.77	0.22	0.07	0.20	0.02	0.15	0.10	0.06
Pyruvate kinase PKM	383.34	381.16	334.20	3.41	6.72	2.35	0.26	0.51	0.51	0.88	0.92	1.41
DNA-binding protein	185.63	242.56	258.81	0.03	0.20	0.07		0.06				
Histone H1.4	116.54	99.24	100.20									
Histone H4	75.59	63.65	67.62	3.51	4.46	1.43	0.29	0.24	0.23	0.38	0.46	0.48
Protein disulfide-isomerase	64.42	47.73	70.53	0.09	0.14	0.01		0.03		0.02	0.09	0.05
E1B 55 kDa protein	63.24	58.20	47.12									
Annexin A2	57.37	53.66	51.90	3.66	0.38	0.80	0.70	1.56	0.92	2.08	1.18	2.23
Peroxiredoxin-2	37.52	33.10	37.38	2.96	0.30	0.27	0.63	1.51	0.25	2.36	1.56	2.28
E1B protein, small T-antigen	28.93	26.99	22.42	0.02	0.03							

10000 ppm — 50th percentile — 20 ppm | 40 ppm — 50th percentile — 0 ppm | 5 ppm — 50th percentile — 0 ppm | 5 ppm — 50th percentile — 0 ppm

***Empty* Capsids**

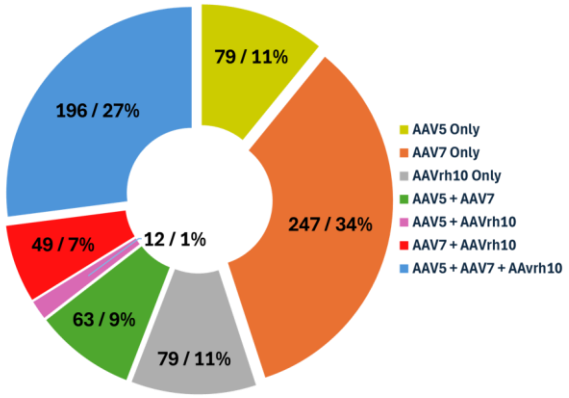

***Full* Capsids**

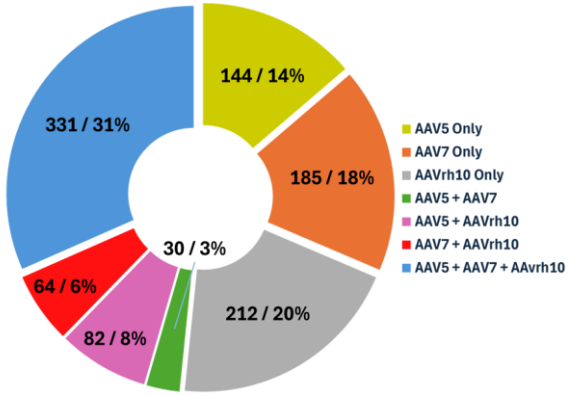

- Ability to separate empty and full capsids affected differentiation of HCP loads, however some specificity was observed.
- Similarly, specificity was observed for the serotypes analysed.
- ‘Problematic HCPs’ were investigated in the resulting LC-MS data to evaluate their clearance, as shown in the heatmap, the majority were cleared by AAVx affinity chromatography.

Summary

- Native MS and CDMS can be coupled with upfront anion exchange chromatography for confirmation of capsid fill state. Partial capsids not observed either by chromatography or MS, thought to be due to GOI size.
- Viral protein separation possible using various chemistries, HILIC method works well and is simple to deploy, however, reversed-phase outperforms for separation of deamidated forms.
- Top-down MS/MS showing strong potential for VP specific characterisation. Combination of different ion activation strategies on tribrid MS instrument enabled excellent N- and C-terminal fragmentation.
- HCP behaviour investigated using throughout the downstream process for HEK293 derived serotypes using Orbitrap Astral. Some specificity identified based on the serotype and capsid fill state, however, AAVx affinity chromatography enables bulk clearance.

Acknowledgements

NIBRT:
Josh Smith, Corentin Beaumal, Sara Carillo, Aaron Richardson, Felipe Guapo, Colin Clarke, Florian Füssl, Lisa Strasser, Silvia Millán-Martín

Thermo Fisher Scientific:
Eugen Damoc, Anna Pashkova, Kristina Srzentic, Tabiwang N. Arrey, Kai Scheffler, Kelly Broster, David M. Horn, Steve G. Milian, Richard O. Snyder

908 Devices:
Erin Redman

ThermoFisher SCIENTIFIC

ENTERPRISE IRELAND

Science Foundation Ireland sfi For what's next

nibrt National Institute for Bioprocessing Research and Training